EXAMINATION OF THE TWO-PHASE FLOW MODEL IN VARIOUS FLOW CONFIGURATIONS

by

Miroslav SIJERČIĆ and Florian MENTER

Original scientific paper
UDC: 533.6.011
BIBLID: 0354–9836, *4* (2000), 2, 5–32

An integrated two-phase flow model including phase interaction is used to examine five particular systems of gas particles flows. The computations have been performed with the CFD software TASCflow3D of AEA Technology. The numerical results of TASCflow3DFLOW have been compared with experimental data and some of them with results from the second code in the project FASTEST of INVENT Computing from Erlangen. There are, of course, still some general problems to be solved for improving calculation efficiency of two-phase flow and to make the numerical codes more efficient in order to allow the calculation of more complex flow in experimentally non-established situation with an acceptable confidence. However, the problems become considerable smaller if consideration is based on proved elementary situations. In general, presented calculation results of test cases showed a quite good agreement with the experimental data. This gives significant contribution to overcome existing uncertainties in two-phase flow prediction. The results for these cases confirmed that the models work properly and that the two software packages in the project produce very similar results.

Introduction

Gas-solid two-phase flow is common in environmental (*e. g.* wind transport of dust) and industrial processes. Gas-particle flows play significant role in some important industrial applications such as pulverized coal combustion and flue-gas cleanup. The suspended flows start to play active roles in some non-conventional applications too. It is recognized as a possible coolant of commercial heavy-duty heat exchangers owing to its excellent heat transfer performance. There are many others reasons for searching the solutions of gas-solid suspension flows. There is no other efficient way to obtain solution of considered problems, but to solve system of simultaneous coupled conservation equations. These solutions offer some data, which cannot be obtained by measurements.

Many computer codes for two-phase flow calculations were developed based on same theoretical models. The numerical modeling using these codes had been applied to develop or improved different processes. Costly experiments are replaced more and more by numerical simulations, reducing in this way costs in product development considerably. On the other hand, during the recent twenty years, development of computer hardware has gone ahead rapidly. Additionally, highly efficient numerical techniques such as multigrid methods have been developed or adopted. They made possible the upgrading of computer codes to be handled by a non-expert user. However, support by means of the set of predictions of similar or basic situations is necessary.

In this work presented and analyzed are some results of the FORTWIHR (Bayerischer Forschung für technisch-wissenschaftliches Hochleistungsrechnen) research project: Numerical Simulation of Multiphase Flows on High Performance Computers. The goal of the project is to enhance the industrial capabilities to simulate multi-phase flows by technology transfer from the academic to the industrial partners. The main areas of activities in the project are the improvement of the physical models and the speed-up of the numerical methods by use of high performance computing strategies (parallelization, vectorization). The improvement of the physical models is achieved by the computation of test cases with the two codes, TASCflow3D and FAST-EST and by a comparison of the results with experimental data. In case that there are significant differences between the codes or in comparison with the experimental data, the models are evaluated and improved models are implemented into the code in question. In the first phase of the project, the emphasis was on questions of numerical optimization of the software, on grid generation and the computation of chosen test cases.

To be useful tool in industrial predictions, a validation of the physical models in the CFD software is required. This is particularly true for multi-phase flows due to their complex nature. In complex flows, it is difficult to evaluate the performance of the multi-phase model, due to the interaction of a number of complicated phenomena, such as complex geometry or higher order turbulence effects. It is therefore essential to validate the models for simple test cases with well-defined boundary conditions and high quality experimental data. Furthermore, the simple geometries allow for a systematic grid refinement and therefore for a separation of modeling and numerical aspects. The chosen test cases represent basic flow situations, which are valuable in order to evaluate the implementation of the particle tracking models in the CFD software. The results for these cases should confirm that the models work properly and that the two software packages in the project produce very similar results. However, in industrial applications the situation is often more complex due to the presence of additional effects, like complex geometry's, swirl and/or heat and mass transfer with additional chemical reactions. One of the central problems from a fluid dynamics standpoint is the accurate prediction of particle flows with swirl, as swirl is frequently used in technical designs to influence the mixing, or de-mixing of the phases (combustion chamber, cyclone, *etc.*). In order to evaluate the performance of the current software TASCflow under those conditions, an additional test case was considered in the study, namely a jet flow with particles in a co-flowing air stream with induced swirl.

Test cases setup

Software: TASCflow3D, Version 2.9, [1], a licensable code based on a conservative finite-volume method, was applied to solve the test problems. TASCflow3D uses a coupled algebraic multigrid method to solve the difference equations arising from the discretization. TASCflow3D offers a choice of various discretization schemes for the convective terms in the model transport equations. In the present calculations, the Modified Linear Profile Skew-Upwind method in combination with the Physical Advection Correction scheme was employed to discretize the momentum equations. This scheme has a spatial truncation error of second order.

Mathematical model: The simulation model treats the flow as two-phase mixture with Eulerian description of the gas phase and Lagrangian description of the particle movements. Phase coupling is achieved on the basis of PSI-CELL model in accordance with which presence of the particle in the flow manifests trough additional sources of momentum in the continuum phase.

Mean flow equations and turbulence model: The mathematical model of continuous phase has been based on the models developed for single-phase flows, but with the corrections due to the presence of particles. The mathematical model of the present study consists of the Reynolds-averaged equations for mass and momentum. In Cartesian coordinate frame, these can be expressed in tensor form as:

$$\frac{\partial \rho}{\partial \tau} + \frac{\partial}{\partial x_i}(\rho U_i) = 0$$

$$\frac{\partial}{\partial \tau}(\rho U_i) + \frac{\partial}{\partial x_j}(\rho U_i U_j) = -\frac{\partial P}{\partial x_i} - \frac{\partial}{\partial x_j}(\tau_{ij} + \overline{\rho u_i' u_j'}) + S_{p,i} \qquad (1)$$

In the above equations, U_i stands for the mean velocities in the x_i – coordinate directions and P is the mean static pressure. Lower case and primed symbols indicate the fluctuating fields. The fluid density is denoted by ρ. The term S_P is the force due to the interaction of the mean flow with the particles. Equation of momentum contains further unknowns in the form of the Reynolds stresses. These must be related to known quantities via a turbulence model before a closed solution of the above equation system becomes possible. The closure of the time averaged momentum equations has been achieved by differential eddy viscosity turbulence model. In the present work, the k-ε turbulence model is used to provide a link between the turbulent transport of momentum and energy and the mean flow properties. The momentum transfer processes in the vicinity of the wall are modeled with wall functions.

Particle tracking model: In TASCflow3D, the phase is considered in a Lagrangian field frame. A Lagrangian tracking model is used to characterize the flow behavior of this phase. The application of the Lagrangian tracking involves the integration of the particle paths through the discretized domain. Each tracked particle represents a parcel of particles that follow an identical path. Because of stochastic character of calculated particles trajectories, large number (several thousand) of random trajectories are neces-

sary to obtain statistically stable solution. Motion of individual particles in the Lagrangian field can be described by the Basset equation, formulated for turbulent flow by Hinze [12]. For non-rotating frames of reference this equation can be written as:

$$m_p \frac{d\vec{u}_p}{d\tau} = C_D \rho \frac{A_p}{2}(\vec{u}-\vec{u}_p)\left|\vec{u}-\vec{u}_p\right| + \\ + \frac{d_p^3 \pi}{6}\rho\frac{d\vec{u}}{d\tau} + \frac{d_p^3\pi}{3}\rho\left(\frac{d\vec{u}}{d\tau}-\frac{d\vec{u}_p}{d\tau}\right) + \\ + \frac{3}{2}d_p^2(\pi\rho\mu)^{0.5}\int_0^\tau \frac{1}{(\tau-\tau')^{0.5}}\left(\frac{d\vec{u}}{d\tau}-\frac{d\vec{u}_p}{d\tau}\right)d\tau' + \\ + \frac{d_p^3\pi}{6}(\rho_p-\rho)\vec{g} + \frac{d_p^3\pi}{12}\rho[\vec{\Omega}\times(\vec{u}-\vec{u}_p)] \qquad (2)$$

In most cases, the last four terms on the right hand side of the equation, namely the pressure forces, forces due to the particle "added" mass, Basset and Magnus forces may be neglected. In the considered flows where the particle density is much greater than the fluid density, equation of particle motion reduces to:

$$m_p \frac{d\vec{u}_p}{d\tau} = \frac{1}{2}C_D\rho A_p\left|\vec{u}-\vec{u}_p\right|(\vec{u}-\vec{u}_p) + \frac{d_p^3\pi}{6}(\rho_p-\rho)\vec{g} \qquad (3)$$

The quantity C_D is sometimes called the friction factor. For the creeping flow ($\mathrm{Re}_P < < 0.1$) around spheres, the drag force is given by the Stokes's law with C_D equals $C_D = 24/\mathrm{Re}_p$, where Re_p is Reynolds number of particle motion relative to the fluid. For higher values of Reynolds number, the values of the friction factor are results of experiments $C_D = (24/\mathrm{Re}_p)C_{cor}$. In TASCflow3D the following expression is used for C_{cor}:

$$C_{cor} = 1 + 0.1315\,\mathrm{Re}_P^{(0.82-0.05\alpha)} \quad \text{for} \quad \mathrm{Re}_p < 20 \quad \text{and} \\ C_{cor} = 1 + 0.1315\,\mathrm{Re}_P^{0.6305} \quad \text{for} \quad \mathrm{Re}_p > 20 \qquad (4)$$

where $\alpha = \log \mathrm{Re}_P$. Particle motion due to turbulent fluctuations is described on the basis of so called stochastic model. Instantaneous equations of particle motion are solved along the random trajectories. Sampling of the instantaneous fluid velocity (sum of averaged and fluctuation) is taken from a Gaussian distribution with a standard deviation equal to the turbulence intensity. The fluid instantaneous velocity components are kept constant during the fluid Lagrangian integral time scale corresponding to the large eddy lifetime. The turbulent velocity, eddy lifetime and length scale based on the local turbulence properties of the flow:

$$u'_f = \Gamma(2k/3)^{0.5};\quad \ell_e = C_\mu^{0.75}k^{1.5}/\varepsilon;\quad \tau_e = \ell_e/(2k/3)^{0.5} \qquad (5)$$

The variable Γ is a normally distributed random number, which accounts for the randomness of turbulence about a mean value. The velocities influence the motion of the observed particle during the defined interaction time. The new fluctuation components are sampled after characteristic time or length scales are exceeded. If in the numerical procedure one takes sufficiently small time interval $\Delta\tau$, the changes of fluid parameters can be neglected in the equation of particle motion, and the exact analytical solution for particle velocity components can be derived:

$$\vec{u}_p = \vec{u} - (\vec{u} - \vec{u}_p^0)\exp(-\Delta\tau/\tau_p) + \tau_p \vec{F}_r[1 - \exp(-\Delta\tau/\tau_p)] \tag{6}$$

where $\vec{F}_r$ is the resultant of forces acting on particle. It presents unit force [N/kg]. The second integration yields the distance of the particle movement.

The dispersed phase is modeled as a set of discrete trajectories with constant particle number flow rate ($\dot{N}_{ij}$) along each trajectory. The effect of the particles on the fluid flow field is provided by the momentum source terms. It is consequence of the force of interaction between fluid and an individual particle. Momentum source term in fluid phase due to particle presence is the results of acting of all particles, which cross the considered control volume, during the residence in this control volume. This source term (*e. g.* for the x-direction) can be represent by:

$$s_{mom}^x = \frac{1}{V}\frac{\pi}{6}\rho_p \sum_i \sum_j \sum_k [(u_{p,ijk} d_{p,ijk}^3)_{inl} - (u_{p,ijk} d_{p,ijk}^3)_{out}]\dot{N}_{ij} =$$

$$= \frac{1}{V}\sum_i \sum_j \sum_k \sum_{\Delta\tau} 3\pi d_{p,ijk} C_{cor}(u_{p,ijk} - u)\Delta\tau \dot{N}_{ij} \tag{7}$$

Boundary conditions: Boundary conditions for the gaseous phase are determined in the same way as for single-phase flow. For the all test cases, the main problem was the inflow boundary condition, where profiles for the mean and the turbulence quantities had to be described. In the case of a constant turbulence intensity and a constant length scale specifications, a non-realistic flow development if turbulent velocity profiles have been obtained. For confined jet, plane flow and swirl flow, the inlet profiles of gas phase velocity components are determined by regression presentation of the tabulated experimental data. For these test cases, the inlet profiles of turbulent kinetic energy were computed from the relations, based on local RMS values of velocity fluctuating components – $k = 0.5(u'^2 + v'^2 + w'^2)$.

In the case of the free jet, the experimental flow configuration ensured fully developed turbulent profiles at the tube exit, which forms the inlet to the free-jet flow. In accordance with this fact, for the description of the inflow velocity and turbulence characteristics, universal profiles for developed flow in a pipe are used. Gas velocity profiles are described by means of the known "1/7" power law: $U/U_{\max} = (1 - r/R)^{0.1428}$. From Blasius equation for a pipe wall shear stress: $2\tau_w/\rho < U >^2 = 0.071 \cdot \mathrm{Re}^{-0.25}$ in which $\mathrm{Re} = < U > D/\nu$ is the Reynolds number of the bulk flow and $< U >$ is the average velocity in the pipe, one gets the friction velocity: $U_\tau = (\tau_w/\rho)^{0.5} = (0.0355 < U >^2 \mathrm{Re}^{-0.25})^{0.5}$.

In the case of the step flow, the dimensions of the inlet length of the test section in the experimental rig were designed to ensure also fully developed flow conditions at the step with respect to the vertical and lateral profile symmetry, mean flow and turbulence quantities. So the profile of inflow velocity was determined as a function of the Reynolds number of the bulk flow (formed with the step height H: $\mathrm{Re}=<U>H/\nu$) in the form of a "1/7" power law.

At high Reynolds numbers in developed turbulent pipe flows, the radial profiles of the turbulent kinetic energy are in non-dimensional form ($k^+ = k/u_\tau^2$) parabolic with a value of 0.8 at the axis and around 3.5–4.5 near the wall (at $y^+ = 30$). Experimental and theoretical investigations of boundary layer flows show that in general, the profile of the turbulent kinetic energy in a developed turbulent flow near the wall can define by the expression: $k = [1 - \exp(-y^+/11)](1 + a_1 z + a_2 z^2)\cdot\mathrm{const.}$ where $z = y_i/y_G$ is the ratio of the current distance from the wall and the lateral coordinate of the edge of the boundary layer. The constants a_1 and a_2 can be calculated from the conditions that $dk/dz = 0$ and $k = k_G$ at $z = 1$, leading to $a_1 = -2a_2$ and $a_2 = 1 - k_G/\mathrm{const}$. From the experimentally established relations $k_G = 0.8U_\tau^2$ and $k/U_\tau^2 = 3.3$ at $y^+ = 30$ we get $\mathrm{const.} = U_\tau^2/0.3$. This approach usually gives good results if it is used for describing inflow boundary conditions and it is here applied to the calculations of the free round jet and flow over backward facing step. For the non-dimensional turbulent kinetic energy dissipation rate ($\varepsilon^+ = \varepsilon R/U_\tau^3$) there is also an "universal" parabolic (probably of forth order) profile. Turbulent kinetic energy dissipation rate at inlet is determined in function of turbulent kinetic energy and dissipation length scale: $\varepsilon = C_\mu^{0.75} k^{1.5}/L_\varepsilon C_\mu$ is the structure parameter of turbulence. The length scale distribution is calculated from: $L_\varepsilon = \min(\kappa y, \lambda\delta)$ with the distance from the inner or outer wall, y, the thickness of the shear layer, δ, and the constants, $\kappa = 0.42$ and $\lambda = 0.14$. Length scale is determined for each slot separately.

Some specific problems appear in the modeling free jets. In general, they arise because of the non-existence of well-defined boundary conditions in the far field, resulting in unexpected difficulties in solution convergence. Special attention should be paid to the boundary conditions, which should be posed in the "quiescent" fluid. For these free boundaries, which separate the flow field from its surroundings, it is possible to fix the values of the variables, or values of their derivatives, or to extrapolate the values of the variables in the vicinity of the boundary. These possibilities can be used for all variables, but because of entrainment not for the velocity components perpendicular to the boundaries. At the inlet, outside the jet region, proper conditions can best be achieved by a constant total pressure boundary condition. It reflects the fact that the fluid entering the domain comes from a domain of constant energy and therefore satisfies the Bernoulli equation. In the neighborhood of the pipe exit, the gradients of the variables were high, leading to solution divergence of the solver. After a few attempts with grid refinements and rearrangements, a portion of the pipe was included in the simulation. A part of the pipe wall became so an internal object in the flow.

The other boundary conditions were: outlet with constant pressure at the outflow plane or with pressure set at a single face in the outflow plane, symmetry in lateral and circumferential direction and standard wall functions at walls.

Boundary conditions for the particles are specified on the wall surface and at the symmetry surfaces of the flow area. It is assumed that the particles reflect off the walls with the degree of elasticity equal to 0.8. The condition of symmetry implies the "reflection" of particles at the surface of symmetry, meaning that every particle crossing the surface of symmetry is balanced by the corresponding crossing of a particle in the opposite direction. Inflow particle velocity data are taken from the experiments.

Numerical grids and convergence

In the frame of the model and code sensitivity examination, for the purpose of testing the consistency of the numerical results, the influence of the number of the particle trajectories was considered. The same order of magnitude of the dimensions of the experimental rigs of the considered test cases, enable some common conclusions concerning particle tracking to be made. Reliable results have been made. Reliable results have been obtained with two thousand trajectories. Calculations with 5000 instead of 2000 particle trajectories have been performed. Starting the calculation from a previously converged solution with a lower number of particle trajectories, the particles disturbed the fluid flow field, but after two or three iteration cycles convergence was again achieved. Calculation results for 5000 trajectories differ from the results with 2000 trajectories much less than 1% for all flow features. This is probably because of the low particle concentration in the flow. The number of particles in the flow is small enough that the motion of the gas is not much affected by the particles. The main difference was in computational time. The necessary CPU time for particle tracking calculations is proportional to the number of particle trajectories. CPU time for particle tracking is not an absolute number. Particle tracking time depends on the number of representative particle trajectories, the frequency of particles injections, the total amount of particles in the flow, the flow configuration, the number of particles captured in the recirculation and the total number of iterations. The total computation time and the number of iterations depend also on the guessed initial profiles. However, in general, the time spent for particle tracking calculations was between 10% and 20%.

In addition, a grid refinement study was carried out. Comparisons of results with 61×3×51, 121×3×81 and 201×3×131 nodes showed only small differences in the solution of the two finer grids. It is therefore assumed that the medium grid is sufficient for the simulations. For a relatively freely guessed initial field of the confined jet with heavy particles, sixty iterative loops were required for convergence. The maximum residuals were less than $5.0 \cdot 10^{-5}$.

In the case of 61×3×51 grid points fifty iteration loops required 259 CPU seconds on Silicon Graphic workstation. In the case of 121×3×81 nodes, 748 CPU seconds have been necessary. In the case of 61×3×51 nodes, 56% of CPU time was consumed for the hydrodynamic variables, 21% for turbulence equations and 20% for the particle tracking calculation. In the case of 121×3×81 nodes, this ratio was 64%: 23%: 11%. For the calculations with 201×3×131 nodes, 2760 CPU seconds were necessary, 65.9% of which

were for the calculation of hydrodynamic variables. About 23% were consumed for the calculation of the turbulence variables and 6.5% for particle tracking.

Two-phase flow in a confined jet

Geometry and flow configuration: The test case of a confined jet flow with particles is considered first. The geometry of the experimental set-up is shown in Fig. 1 [6].

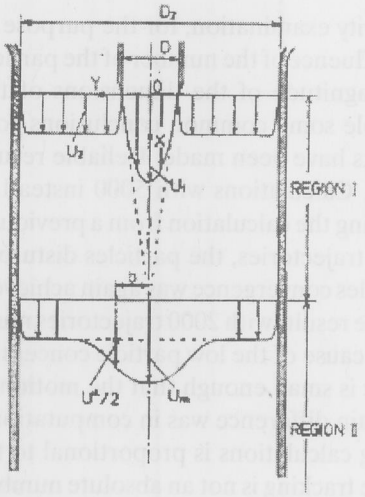

Figure 1. Confined jet configuration

A particle-laden core jet enters a co-flowing air stream with different velocity. The exit diameter of the central pipe is $D = 13$ mm and the outer pipe has a diameter of $D_2 = 60$ mm. The exit velocity at the centerline of the inner pipe was set at 30 m/s and the average velocity of the outer co-flow was around 15 m/s. This condition does not produce a recirculation region. The experiments were conducted under atmospheric conditions and with two different types of particles. The particle mean diameter was 80.1 μm for light particles and 64.4 μm for heavy particles. The particle densities were 280 kg/m^3 and 2590 kg/m^3 for light and heavy particles respectively. Corresponding the particle mean volume fractions were same $1.4 \cdot 10^{-4}$, but the mass loading ratios were 0.033 for light particles and 0.33 for heavy particles. The measurements of mean and fluctuating velocity components are given at the inlet and at three axial sections in the developing region [2], [6]. The initial profile of the turbulent kinetic energy had to be determined indirectly, because the third fluctuating velocity component is not known. However, the main problem was the determination of the turbulent kinetic energy dissipation rate at the inlet cross section. This quantity can have a strong effect on the flow development downstream and is therefore a sensitive parameter. The calculated flows can be considered as simple, but elementary flows are often more delicate for predictions than complex flows, where many facts can be on the inside hidden. On basis of cases considered here, accuracy and reliability of the results do justify using the code also for complex situations with heat and mass transfer.

Results for flow with light particles: The comparison of the computed and the experimental axial mean velocity at two different downstream locations of the flow ($x =$ $= 130$ mm and $x = 260$ mm) is shown in Fig. 2. There are some differences between the computations and the experiments mostly in terms of the spreading rate of the core jet. The reason for the higher spreading rate of the computed results could be the influence

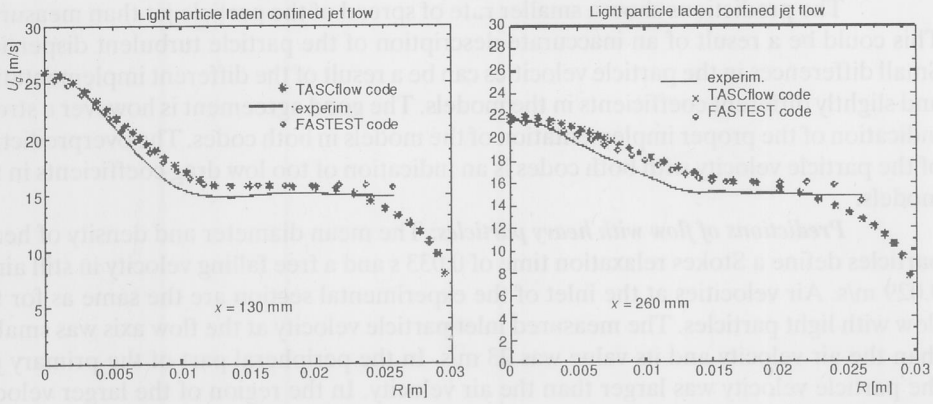

Figure 2. Comparison of gas phase axial mean velocity profiles in the two-phase confined jet (light particles)

of the inlet conditions on the results. As all inflow quantities are not available from the experiments, there is some arbitrariness in the specification of the inlet profiles. This might lead to differences between the simulations and the experiments.

In order to further examine the differences between the computations and the experimental data, in the same figure the results of TASCflow where compared with solutions produced with FASTEST using the same boundary conditions.

In addition, the grid was the same for both codes. The results from both codes are very similar. Figure 3 shows a comparison of the computed and the experimental particle velocities. The agreement with the experiments is very good, considering the differences in the mean flow, which affect the particle trajectories.

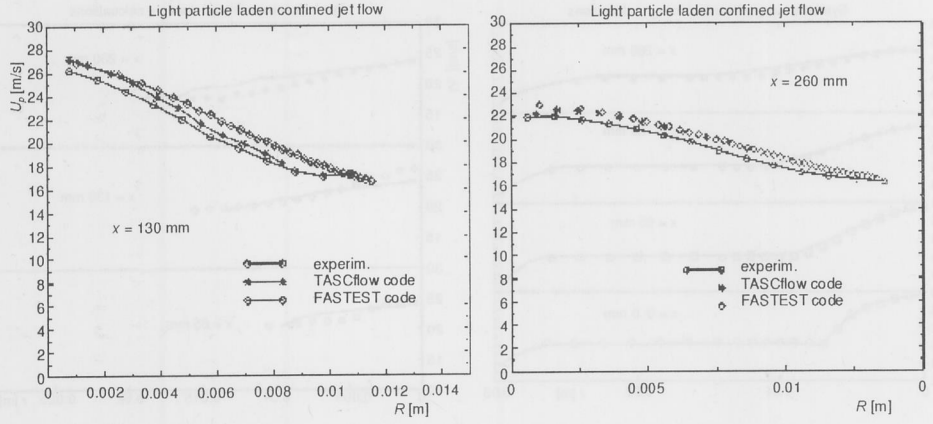

Figure 3. Comparison of particle phase axial mean velocity profiles in the two-phase confined jet (light particles)

The predictions show a smaller rate of spread of the particle jet than measured. This could be a result of an inaccurate description of the particle turbulent dispersion. Small differences in the particle velocities can be a result of the different implementation and slightly different coefficients in the models. The good agreement is however a strong indication of the proper implementation of the models in both codes. The overprediction of the particle velocity with both codes is an indication of too low drag coefficients in the models.

Predictions of flow with heavy particles: The mean diameter and density of heavy particles define a Stokes relaxation time of 0.033 s and a free falling velocity in still air of 0.029 m/s. Air velocities at the inlet of the experimental section are the same as for the flow with light particles. The measured inlet particle velocity at the flow axis was smaller than the air velocity and its value was 23 m/s. In the peripheral part of the primary jet, the particle velocity was larger than the air velocity. In the region of the larger velocity of the gas phase, particles accelerate due to their weight, with the tendency to reduce the velocity of the gas stream. In the region of smaller gas phase velocity, particles moderately decelerated due to the influence of the fluid stream. In case of equal local velocity of both phases, the velocity of the particles relative to the gas increases due to their inertia with a tendency to reach the magnitude of the free fall velocity plus the gas velocity. The calculated results captured this behavior. Figure 4 shows the mean gas phase velocity in comparison with the experiments. The agreement with the data is similar to the comparison with the light particles. This is to be expected, as the particles have only a limited influence on the gas phase. The result of the calculations on the fine grid did again not differ by more than 1% from the results on the coarse grid. Figure 5 shows the comparison of the particle velocities. Again, the agreement with the experimental data is good, considering the gas phase velocity differences.

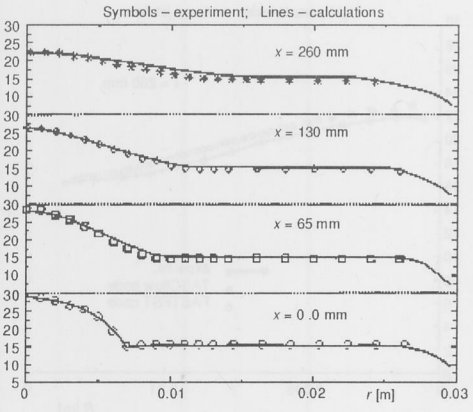

Figure 4. Gas phase mean velocities in the confined jet (heavy particles)

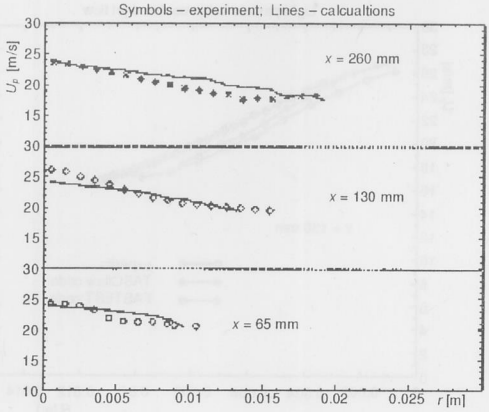

Figure 5. Particle phase mean velocities in the confined jet (heavy particles)

Particle laden round free jet

Flow feature description: The second subject of testing and discussion was a circular particle air jet flowing in the direction of gravity and discharging into a stagnant surrounding. The experimental results contain the complete data set of hydrodynamic flow characteristics including turbulence data for both phases. The particles were injected at the beginning of the vertical pipe. The particles and air stream mix during their flow through the tube. The tube is 1 m long and has an inner diameter of 0.013 m. At the tube outlet (flow field inlet) the mixture reaches fully developed velocity and turbulence profiles. Particles of mean size around 64 μm with nominal density $\rho = 2560$ kg/m^3 were used. The size distribution of the particles ranges from 40 μm up to 120 μm. The data set of inlet boundary condition comprises: centerline air velocity equal 30 m/s, particle centerline velocity equal 26.2 m/s, particle mass loading equal 0.3 kg/kg. For three different downstream locations of the flow ($x/D = 10$, $x/D = 20$ and $x/D = 30$) experimental data sets are provided.

Result of numerical calculations: Free round jet predictions often suffer from the deficiencies in predicting jet spreading rates when calculated with the k-ε turbulence model. It is more well known fact. This was also the case in the presented calculations of a free round particle laden jet. A comparison of the computed gas phase velocity with the experimental data showed some disagreement when the computations have been performed with the standard coefficients for the k–ε model. The higher spreading rate obtained by calculations can be observed in the reduction of the centerline velocity in the simulations. In the present calculation, the mismatch is quite substantial, with differences of around 20%. A frequently used remedy for this deficiency is the change in the coefficient of the k-ε model. Many different modifications have been proposed. Good agreement could be achieved by the correction due to [8]: $C_{\varepsilon 1} = 1.14 - 5.31(Y_{0.5}/U_m)(dU_m/dx)$. In the present case, the constant value of $C_{\varepsilon 1} = 1.55$, instead of $C_{\varepsilon 1} = 1.44$ was used. With the modification of one of constants of turbulence, model good agreement with the experiment has been obtained. The same effects were observed by the project partners in Erlangen, who used an even higher coefficient of $C_{\varepsilon 1} = 1.60$ to match the gas phase velocity field. Presented results are for the computation based on the modified coefficient.

A comparison of the experiments with the predictions by the two different numerical codes is shown in Figs. 6 and 7. The profiles of the gas and particle veloci-

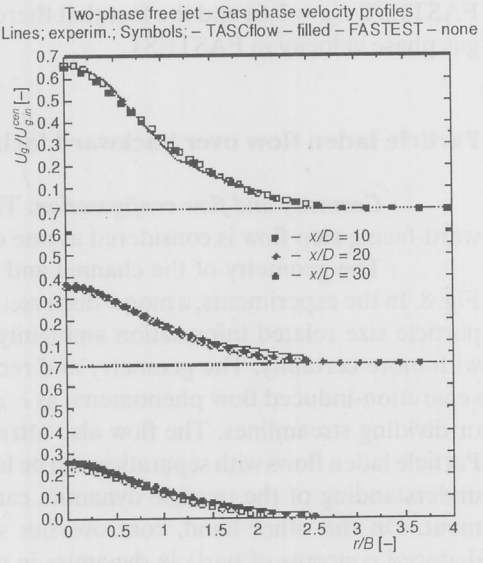

Figure 6. Comparison of gas velocity profiles for free jet

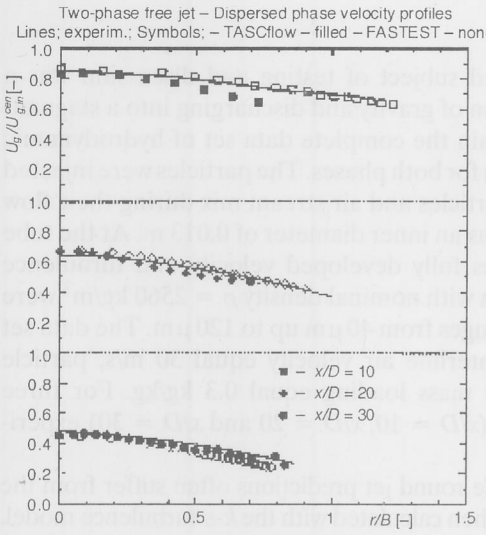

Figure 7. Comparison of particle velocity profiles for free jet

ties are normalized with the inlet centerline gas velocity. The radial coordinate is normalized with the jet width of each profile, since no absolute radial coordinate was given in the experimental data. The jet width B represents a local radial distance from the jet axis at which the mean velocity is equal to one half of the centerline velocity at the same axial location. Both codes give very similar results and are in good agreement with the experimental data.

The particle velocities are significantly higher than the gas phase velocity, due to the higher inertia of the particles. The particle-tracking module correctly predicts this effect. It can be seen from Fig. 7 that the agreement of the predicted particle velocities with the experimental data is good. This is partly a result of the modification of the turbulence model and the resulting high accuracy of the mean gas phase velocity. Slight differences between the codes can be attributed to the slightly different modification of the turbulence coefficient (TASCflow $C_{\varepsilon l}$ = 1.55; FASTEST $C_{\varepsilon l}$ = 1.6) and the fact that there is no comments of the particles to the mean gas phase velocity in FASTEST.

Particle laden flow over backward facing step

Geometry and flow configuration: The particle dispersion in a single-sided backward-facing step flow is considered as one of the test cases.

The geometry of the channel and the illustration of the flow field are given in Fig. 8. In the experiments, a mono-dispersed particle size distribution was used to exclude particle size related information ambiguity. This enables the modeling to be analyzed with more certainty. The geometry and recalculation of the flow enable the analysis of separation-induced flow phenomena, as *e. g.* the determination of re-attachment length or dividing streamlines. The flow also attracts attention from a practical point of view. Particle laden flows with separation can be found in many technical processes and a better understanding of the particle dynamics can increase the efficiency of technical equipment. On the other hand, controversies still exists between the mostly theoretically deduced concepts of particle dynamics in complex turbulent flows. So every particular numerical study, which can be supported by experimental results, is valuable. The experiments were carried out in a closed-loop wind tunnel with a test section made

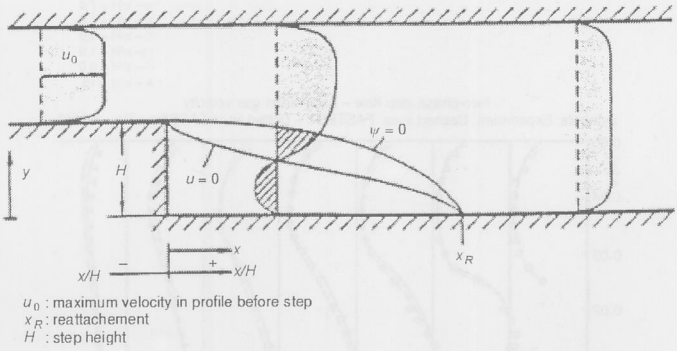

Figure 8. Sketch of flow with a sudden enlargement

of glass. An expansion ratio of the test section was 1:2. The inner width of the test section was 500 mm, the step height was $H = 25$ mm and the channel height after step was 50 mm. At the channel inlet, fully developed turbulent flow conditions were ensured. The highest possible inlet velocity was 50 m/s. Particles of almost uniform size were used for the investigation. The density of the particle material was $\rho = 1500$ kg/m^3. The particle number density in the flow was relatively low $10^2 - 10^3$ cm^{-3}. At this particle concentration level, the fluid field deformation is negligible. The experimental data set provides time averaged flow velocities for gas and the cloud of particles as well as turbulence intensity in axial direction at twelve axial locations.

Numerical results and comparison with experiments: The flow of the present test case shows several important hydrodynamic effects (sharp velocity change, recirculation, *etc.*), which may have strong influence on the dispersed phase motion and on the corresponding mechanical processes and facilities. The contour plot of the calculated streamlines (Fig. 9) gives an illustrative picture of the velocity profile development after the sharp widening of the channel cross section.

Figure 9. Stream lines for the step flow

The comparison of the computed results to the experimental data is shown in Figs. 10 and 11. The predicted velocity profiles of the continuous phase show a reasonably good agreement with the experimental data. The gas velocity profile development is somewhat faster in the model than in the experiment. With the approaching of the fully developed turbulent flow downstream of the step, the velocity agreement improves.

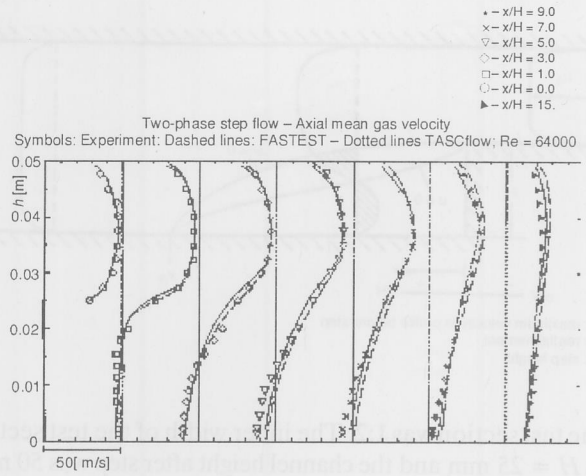

Figure 10. Gas phase axial mean velocity profile development behind the step

Local velocities of the dispersed phase were determined as the mean values of the velocities at all trajectories crossing the exit boundary of the control cell and at the point of that crossing. Velocity profiles of the dispersed phase (Fig. 11) show that the velocity decrease along the channel is slower than that of the continuous phase, which is a consequence of the particle inertia. When calculating the flow with very smaller particles (d_p = 10 μm) this effect does not appear, and the particle velocities follow closely the local gas flow velocity.

In Fig. 11, it can be observed that in the region of the main flow the agreement of the velocities is good. In the region of the recirculating flow, the particles do not reach the wall. Therefore, in the cross-sections close to the step the model gives particle velocity

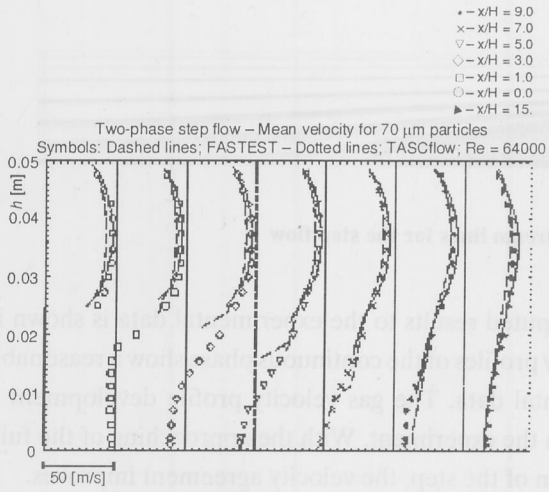

Figure 11. Particle phase axial mean velocity profiles development behind the step

profiles only up to the edge of the recirculating zone. It was examined if the coarse grid or the insufficient number of representative particle trajectories were the cause for this miss-match. A calculation with 8000 particles did not show a difference in the obtained results. Again, there were not particles in the recirculation zone with the finer grid. Additional studies based on different inlet velocities, dimensions and particle flow rates, number of control volumes and particle trajectories were performed. The main difference in the simulation came from the lower velocity level (Re = 15000) at the inlet.

This modification did lead to particles inside the recirculation zone. The agreement with experiments concerning the particle velocities and distribution were acceptable, as can be seen in Fig. 12. The results are also in agreement with the diagram of particle concentrations (Fig. 13).

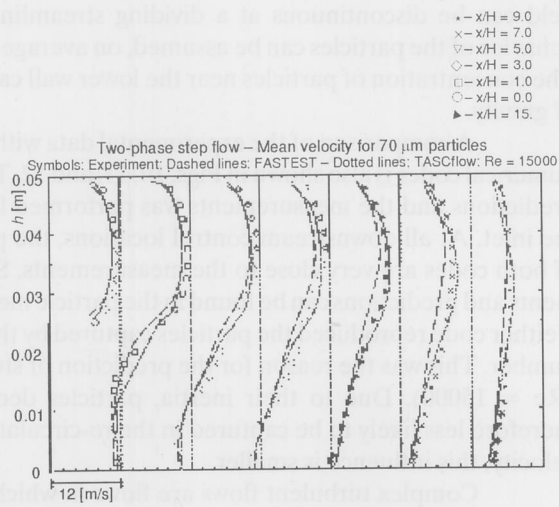

Figure 12. Mean velocity profiles for 70 μm particles behind the step with Re = 15000

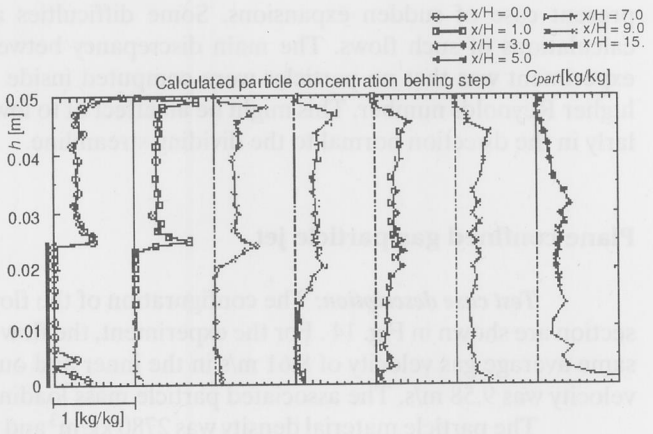

Figure 13: Particle concentration behind the step (Re=15000)

The particles of major interest in the industrial applications are usually called heavy particles, small particles of high density such that they have a free-fall velocity on the order of fluid rms velocity. Complex flows found in industrial processes can have loading of these particles large enough to change the turbulent character of the flow. Particle concentration influences flow characteristic in two ways: through its level and its gradient. Experimental evidence shows that particles tend to migrate from regions of high strain into less active region. Similarly, in the process of turbulent fluctuation particles tend to migrate in the field of lower concentration and make concentration field even. Of course, they have sometimes prevented in this "intention" by other effects. Predicted particle concentration field in this work looks logical and illustrative. The local values of particle concentrations are determined as the mean value of the particle number flow rate trough the considered control volume. Because of that, the particle concentration field can be discontinuous at a dividing streamline. The influence of gravity on the behavior of the particles can be assumed, on average, to act independently of turbulence. The concentration of particles near the lower wall can be a consequence of the influence of gravity.

A comparison of the experimental data with the predictions by the two different numerical codes is also shown in Figs. 10, 11, and 12. The comparison of the two numerical predictions and the measurements was performed for six cross sections downstream of the inlet. At all downstream control locations, the predicted gas and particle velocities of both codes are very close to the measurements. Some differences between measurements and predictions can be found in the particle mean velocity in the recirculation zone. Neither code reproduced the particles captured by the recirculation at the high Reynolds number. This was the reason for the prediction of step flow at a lower Reynolds number (Re = 15000). Due to their inertia, particles decelerate slower then gas. They are therefore less likely to be captured in the re-circulation zone. At the lower level of inlet velocity, this influence is smaller.

Complex turbulent flows are flows in which the turbulent energy and the time scale change significantly with the location. Examples of complex flows include the present case of sudden expansions. Some difficulties are often encountered in the calculations of such flows. The main discrepancy between the computations and the experiment was that no particles were computed inside the recirculation zone for the higher Reynolds number. This might be an effect of to low turbulent dispersion, particularly in the direction normal to the dividing streamline.

Plane confined gas-particle jet

Test case description: The configuration of the flow and the geometry of the test section are shown in Fig. 14 . For the experiment, the flow rates were adjusted to give the same average gas velocity of 8.61 m/s in the inner and outer channels. Average particle velocity was 9.58 m/s. The associated particle mass loading was 0.00253 kg/kg.

The particle material density was 2780 kg/m^3 and the mean diameter of particles was 45 μm. Using laser-Doppler anemometer, Sommerfeld [11] reported measurements

of the phasic flow properties in a two-phase, air-particle turbulent flow in rectangular wide channel.

Result of numerical calculation: One of the test cases already considered was confined two-phase round jet. The predicted gas phase axial mean velocities showed rather good correlations to the experiment in the core region of the flow. In the peripheral region of the flow, the results of the calculations were not so close to the experiment. The annular stream showed in the experiment tendency to keep flat inlet profile at unusually long distance. Because of that, there were some confusion concerning the interpretation of conclusions. Is it a question of shortcomings of measurement or software imperfection? As a similar test case, plane confined jet was selected to answer this question.

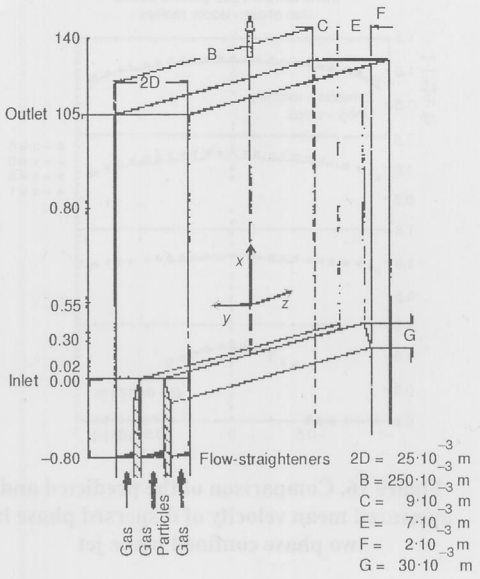

Figure 14. Test section of two-phase plane flow

Model prediction and comparison with experiment [11] for gas phase mean velocities are presented in Fig. 15, which shows the velocity profiles which are normalized with the aid of the averaged inlet velocity. It is observed that the predicted mean velocity is in quite good agreement with experimental data. At the outlet location where the flow is again fully developed, the model predictions

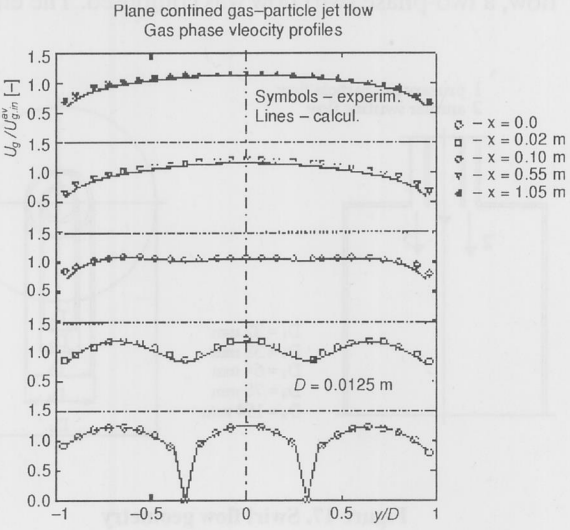

Figure 15. Comparison of the predicted and measured mean velocity of gas phase in two phase confined plane jet

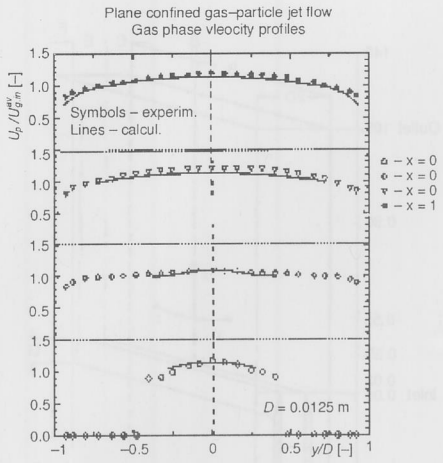

Figure 16. Comparison of the predicted and measured mean velocity of dispersed phase in two phase confined plane jet

are somewhat lower than the experimental data. This difference may be to the fact that the present results of calculations are for two-dimensional vertical channel, while the experimental results for flow with three-dimensional effects with influence of two mutually perpendicular boundary layers. The particle mean velocity profiles are compared with experimental data in Fig. 16. It is observed that the agreement between the measured and predicted mean particle velocity is also very good. A comparison of the particle mean velocities in the near the inlet plane shows again the lower rate of spread of the numerical simulations, indicating somewhat weaker particulate phase model sensitiveness on turbulent diffusion. In general, the solution gave acceptable results for flow field of dilute flows of gas-solid mixture in two-dimensional vertical channel. These results show that the present code can predict the features of the two-phase flow in a duct.

Two-phase swirl flow

For the purpose to confirm the conclusions in the case of one more complex flow, a two-phase swirl flow was computed. The emphasis in this case is on the influence of swirl on the mean flow and particle dispersion. This is a very important effect with strong relation to industrial applications.

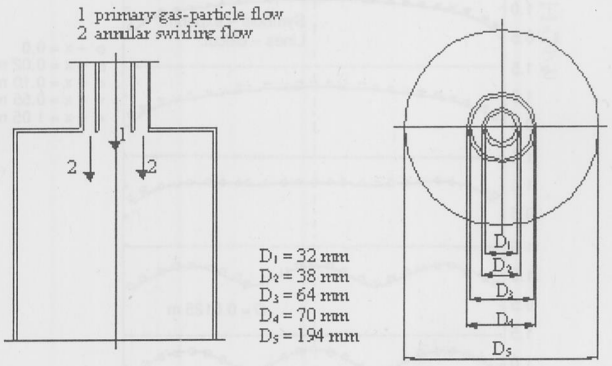

Figure 17. Swirl flow geometry

Flow configuration: The experimental results for this test case were obtained at LSTM (Lehrstuhl für Strömungsmechanik), University at Erlangen [4]. For the study of swirling two-phase flow, a vertical test section with a downward flow was chosen. The geometry of the test section is shown in Fig. 17. A particle-

-laden primary core jet enters a co-flowing air stream or the secondary swirl annular flow. Swirl component is only present in the secondary inlet issuing from the annular slot, and the particles are only issuing from the primary central inlet. The mass flow rates of primary gas jet was 9.9 g/s. The mass flow rates of secondary jet was 38.3 g/s. Mass flow rate of the particles was 0.34 g/s. Particle mean diameter was 45.5 μm. Particle material density was 2500 kg/m^3 . The associated particle mass loading was 0.034 kg/kg. Using laser-Doppler anemometer, Sommerfeld reported measurements of the phasic flow properties in a two-phase, air-particle turbulent flow in circular tube. The measurements of mean and fluctuating velocity components are given at the inlet and at six axial sections along the pipe. Illustration of the flow development on basis of prediction results is given in Fig. 18.

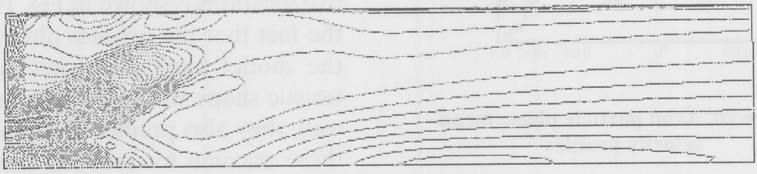

Figure 18. Swirl flow contour lines in radial cross section

The inlet profiles are given for the channel cross section immediately after the fluid inflow from the core pipe and annular slot. Unfortunately, the inflow conditions are not specified completely in the experimental data. Some of the values are missing in particular points and have to be interpolated.

Numerical predictions and results: In the research of turbulent swirling flows, the emphasis is placed mainly on the analysis of recirculating swirling flows due to the wider area of application. Its importance derives from its application to enhance the flame stability in industrial furnaces as well as for particle separation from a fluid stream in cyclones. The flow is strongly influenced by specific effects caused mainly by centrifugal and Coriolis forces. The aim of this work is to analyze the feasibility of the prediction of swirling flow, based on a comparison of the experimental results with the results obtained with the mathematical model. Model predictions for the velocity com-

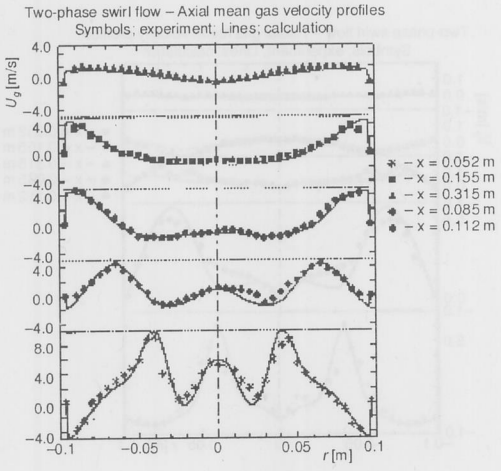

Figure 19. Development of axial gas mean velocity profiles

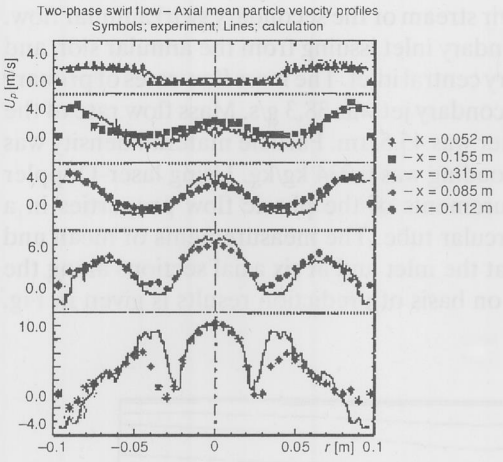

Figure 20. Axial particle phase mean velocity profiles

ponents of the mean gas and particle velocities are presented and compared with the experimental results for five different downstream locations of the flow (x = 52 mm, x = 85 mm, x = 112 mm, x = = 155 mm and x = 315 mm). Radial distributions of mean axial, tangential and radial velocities of both phases have been analyzed. The results are presented in Fig. 19 to Fig. 24.

The comparison of the computed and experimental axial mean velocity at these five locations is shown in Fig. 19. Besides the fact that the profiles obtained using the model have the expected characteristic shape with a maximum near the wall, they also predict the movement of these maxima towards the axis. Due to the influence of the walls, the tangential velocity decreases (Fig. 23) along the channel. The profile spreads and the maximum moves to increasing radii at the downstream locations. The model predicts this development correctly. The radial velocity (Fig. 21) decreases along the axis. The calculation yields a qualitatively correct picture of the velocity development and a relatively good quantitative agreement of the profiles with the experimental data. Certain disagreements of the calculated profiles with the experimental data can be seen in the descending part of the radial profiles. Figures 20, 22, and 24 show a comparison of the computed and the

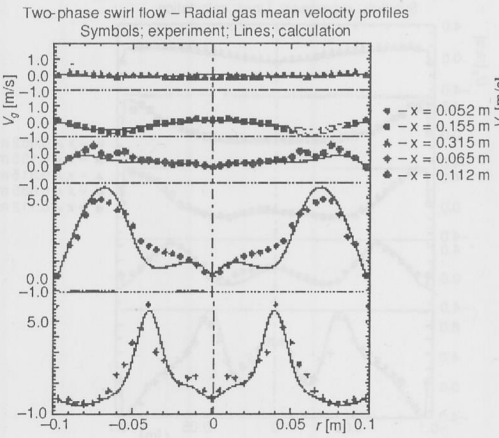

Figure 21. Development of radial gas mean velocity profiles

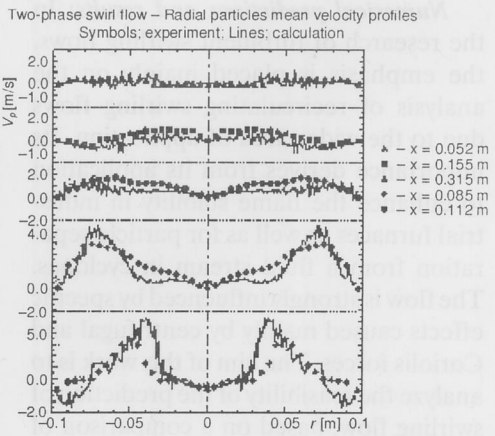

Figure 22. Radial particle phase mean velocity profiles

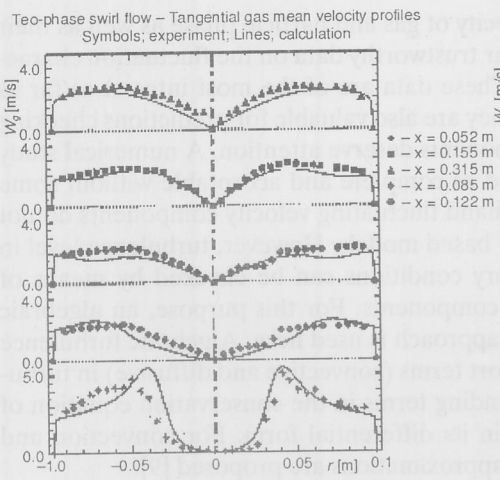

Figure 23. Development of tangential gas mean velocity profiles

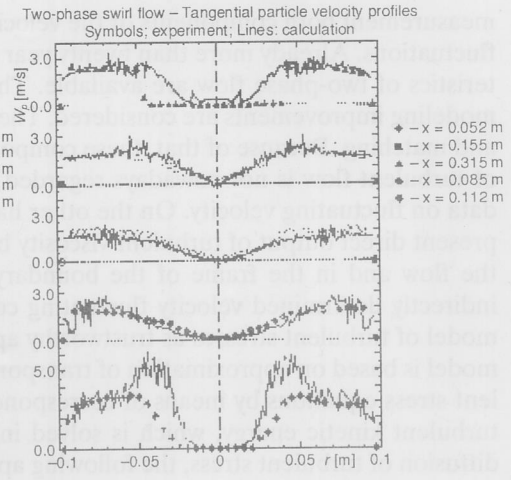

Figure 24. Tangential particle phase mean velocity profiles

experimental particle velocities. Considering the differences in the mean gas flow and the complexity of the flow, the agreement with the experiment is good. The predictions show a somewhat smaller rate of spread of the particle jet than measured.

Imperfections of the physical models in a CFD code need not to be expressed in the case of relatively simple flow configurations. However, in the case of complex flows, different effects are often "multiplied" and become especially pronounced. Because of that, the most meaningful evaluation of the performances of a numerical program is possible in the case of the simulation of flows with complex physics in simple geometries. A two-phase turbulent flow with strong swirl incorporates practically all-physical elements, which make the hydrodynamic prediction of this class of flows complicated. This was the reason for the selection of the present test case. In general, the agreement between the predictions and the experiments was quite good. The prediction gives useful information about the flow structure and the particle motion. This computer code could therefore be successfully applied as a design tool for developing innovative gas-solid cyclone separators or coal-fired cyclone burners *etc.*

Turbulence properties in the two-phase flows

There is still a lack in knowledge about some physical processes in turbulent two-phase flow and therefore their description in the frame of mathematical modeling still needs to be improved. Contemporary optical methods enable us to get new insight into two-phase flow structure. With the very sensitive laser device, the evolution of particle systems has been studied. A laser-Doppler anemometer has employed for

measurement both components of the velocity of gas and particle phase as well as their fluctuations. Already more than twenty year trustworthy data on the fluctuation characteristics of two-phase flow are available. These data are of the most interest as far as modeling improvements are considered. They are also valuable for predictions checking and matching. Because of that, these components deserve attention. A numerical study of turbulent flow is not nowadays regarded as complete and acceptable without some data on fluctuating velocity. On the other hand fluctuating velocity components do not present direct output of turbulent viscosity based models. However, turbulence level in the flow and in the frame of the boundary conditions can be checked by means of indirectly determined velocity fluctuating components. For this purpose, an algebraic model of turbulent stresses as trustworthy approach is used here. Algebraic turbulence model is based on approximation of transport terms (convective and diffusive) in turbulent stress equations by means of corresponding terms in the conservation equation of turbulent kinetic energy, which is solved in its differential form. For convection and diffusion of turbulent stress, the following approximations are proposed [9]:

$$\frac{D\overline{u_i'u_j'}}{D\tau} = C_{ij} = C_k \frac{\overline{u_i'u_j'}}{k}; \qquad D_{ij} = D_k \frac{\overline{u_i'u_j'}}{k} \tag{8}$$

where C_k and D_k are convective and diffusive term in turbulent kinetic energy equation:

$$C_k - D_k = G_k - \rho\varepsilon \tag{9}$$

In such a way one comes to general form of algebraic stress model:

$$\frac{\overline{u_i'u_j'}}{k}\left(\frac{G_k}{\rho} - \varepsilon\right) = \Pi_{ij} + \Phi_{ij} - \varepsilon_{ij} \tag{10}$$

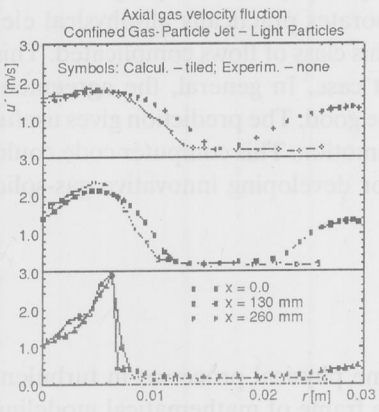

Figure 25. Streamwise turbulence intensity of the gas phase in two two-phase jet with light particles

Between different suggestions, the model has based on algebraic relation proposed by Launder [10]. With simple algebra, the set of algebraic relation, which describe turbulent stresses of continuous phase, has been obtained [17].

Predicted velocity fluctuations: For the demonstration the model's capability to predict Reynolds stresses, the confined jet with light particles (the test case in which some dubious had appeared) and the similar confined plane flow have chosen. The comparisons between experiment and numerical prediction of turbulent fluctuating components as well as turbulent shear stress of gas phase of the confined round jet are shown in Figs. 25, 26, and 27. The associated fluctuations of the velocity components are simulated reasonably well. With re-

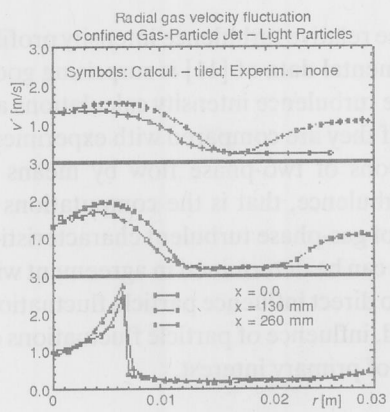

Figure 26. Transverse turbulence intensity of the gas phase in two two-phase jet with light particles

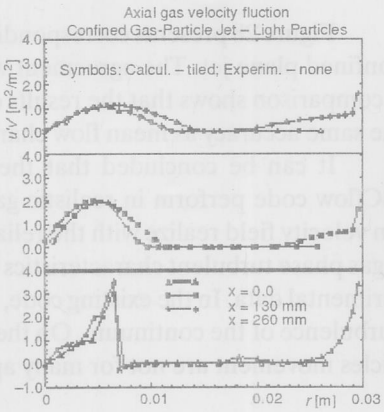

Figure 27. Reynolds shear stress of the gas phase in two two-phase jet with light particles

gard to homogeneous k-ε turbulence model, the predicted turbulent shear stresses are in quite good agreement with the experiment. The turbulent intensity profiles of the gas phase show disagreements with experiments in the wall region just like the mean velocity. The shape of the turbulence intensity as well as the shear stress profiles deviate from those obtained in the experiment in the near wall region. The predicted turbulence normal and shear stresses are higher then the experimental values. Reynolds stress should to increase with approaching wall. Because of that, it looks like a doubt in measurement mistake to have some basis.

The presence of particles in the flow introduces some changes in the flow characteristics. Particles movements are under influence of gas flow and vice versa, particles movements influence on the flow of continuous phase. Solid particles in low turbulence flow with large slip velocity promoted turbulence. The presence of particles in highly turbulent flow made its turbulence isotropic and reduced Reynolds shear stress. In turbulent flows, particles are dispersed by stochastic interaction of turbulence with particles. The velocity fluctuations of particle phase are consequence of gas turbulence. In many cases, they are considerable lower than the fluctuations of the gas phase. Light particles follow the turbulent fluctuations of continuous phase and because of that, fluctuations of light particles are relatively pronounced. In the frame of particle tracking of the stochastic model of dispersed phase, instantaneous velocity components are determinate. Therefore, particle velocity fluctuations could be determinate directly as the variance of particle velocities along the random trajectories. It has been done so in the considered case of confined two-phase jet with light particles. Obtained values of fluctuating velocities were only 30% of those measured in the experiment but they evidently do not strongly influence the calculation of mean flow field.

Figure 28 presents corresponding gas phase relative turbulence intensity profiles of confined plane jet. The agreement with experimental data of [11] is surprising good. The comparison shows that the results of gas phase turbulence intensity calculations are of the same accuracy as mean flow characteristics if they are compared with experiment.

It can be concluded that the computations of two-phase flow by means of TASCflow code perform in realistic gas phase turbulence, that is the computations of mean velocity field realize with the reliable values of gas-phase turbulent characteristics. The gas phase turbulent characteristics themselves can be determined in agreement with experimental data. In the existing code, there are no direct influence particle fluctuations on turbulence of the continuum. On the other hand, influence of particle fluctuations on particles movement are not for many applications of primary interest.

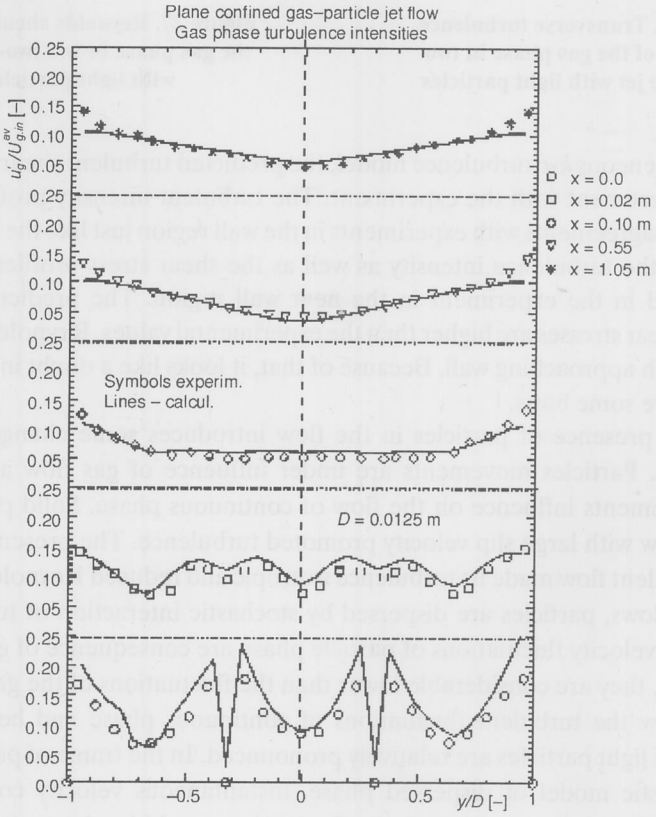

Figure 28. Relative turbulence intensity in two phase confined plane jet

Some common and general characteristics of test cases predictions

Experimental determination of turbulent flow characteristics of the two-phase flow is never simple problem, even for the simple cases. Due to the difficulties in producing full-scale experimental data for complex flows, numerical methods are generally calibrated and tested against experimental data of some simpler configurations. These cases are closer to the theoretical aspect of the problem and eventually mistakes can be easier isolated. Particular effects can be separated and efficiently analyzed. The same can be said for the parts of the program. The influence of a consistent grid refinement can be effectually examined. Optimization of the calculation organization and introducing of new ideas can be performed with success. Due to the similarity with real situations, the result of testing the basic flow can be used with confidence for the applications in the prediction of practical problems. From an applications viewpoint, there remain the specific problems for every case but they are considerable smaller if consideration is based on proved elementary situations.

The considered test cases comprise some important and very delicate elements: mixing layer, sudden expansion of flow cross section, flow separation and free boundary without forced inflow or outflow. These elements are important for many applications. The test cases are in same time fundamental (or elementary) and complex. Calculations were carried out also for some limiting cases: (1) flow with very light particles, when the dispersed phase almost completely followed the fluctuations of the gaseous phase, and (2) flow with heavy particles, where particle inertia proved to be dominant and influence of the turbulent diffusion was insignificant. An increasing particle loading results in stronger coupling between phases and gas flow will be influenced more than in the case of lower particle loading. How the flow field will be changed depends also on the particle size. In the case of larger particles added to the flow, the particle jet will remain almost straight, since the particle relaxation time is much longer than characteristic time length of the considered flow field. The calculation results take notice of these effects. Because of that, these flows deserved to be analyzed and verified, pointing out to the possible model improvements.

The performances of TASCflow code in complex situation have been investigated on the configuration of a swirling particle laden coaxial flow issuing into a sudden expansion chamber. The comparison of the predictions and experiments has effectively concentrated upon looking at mean velocity profiles as main output of practical importance. Turbulent characteristics (turbulence intensity) that could be compared are obtain indirectly during the calculations, and because of that and their objectively less practical importance, to them are paid less attention.

Due to complexity of turbulent gas-particles flows and the difficulty both in numerical modeling and measurements, some problems still remain to be solved before the contemporary computer codes can finally always give reliable results for designing engineering facilities and can be used with confidence in unknown and experimentally not-established situation. This series of test cases calculations had to give contributions to the actual aspirations in this field.

There is still no confirmation about approach for particle motion solution. There is *e. g.* a statement [13] that model based on the "particle tracking concept" is incorrect because it neglect the transport process of particle Reynolds stresses. In spite of that prevails opinion that Lagrangian approach is closer to the physical reality and gives more information (trajectories, particle residence time in considered control volume, *etc.*) necessary for more accurate prediction of particle motion in the turbulent field. Numerical techniques for calculating the mean properties of particle-laden flow were reviewed by Crowe [14], who also points out the advantages of the trajectory model for calculating the convection of the particles and the mean coupling between the particles and the fluid. A comprehensive review of contemporary Lagrangian model used to predict particle motion in turbulent flows is given *e. g.* by Graham [15].

Gas-particle flows are characterized by properties of the particles and by properties of the turbulent gas flow that caries the particles. Turbulence is a key element in almost all-practical flow. The presence of particles in the flows causes turbulence modulation. Particles can cause both reduction and enhancement of turbulence of continuous phase. Momentum exchange between fluid and particle cloud can distort streamlines in the carrier phase, modify the mean velocity field and in this way indirectly change rate of turbulence production or decay. The particles cause a modification of the velocity gradients in the fluid phase and an associated change in turbulence generation. Turbulence motion damps by the drag force on the particles, but in the same time, wake turbulence behind each particle is generated.

Although the equation of motion for a solid particle in a gas flow looks like a simple linear ordinary equation, it is a complex nonlinear expression. One must know the particle trajectory to calculate the drag on the particle, and the drag must be known for finding the particle trajectory. The problem encountered when trying to calculate particle motion is determination of the statistics of the fluid along the trajectory. It brings us to the question of turbulent dispersion in two-phase flow. Except for flows with very high loading of particles, it is the interaction between the turbulent gas flow and the particles that defines the character of the flow. The development of our understanding and ability to predict particle transport and diffusion in gas solid flows is directly linked to our understanding of turbulence.

In TASCflow3D code, the stochastic trajectory model is used to account for the gas-particles turbulent interactions. There are a very large number of variables, which affect turbulent fluid-particle interaction. Random sampling fluctuation velocities in a non-isotropic turbulence field could be sometimes rough approximation of irregular and unsteady turbulent phenomena. To take into account spatial and temporal effects of turbulence, correlation probably should be included into the random sampling. In spite of those theoretical shortcomings, quite well solutions, especially in regular geometry, have obtained with existing model. Because of that, one could conclude that particle dispersion in uniform flow field is relatively well understood. To complete our understanding of particle dispersion in practical flow, experiments need to be done that confirm existing model or give new idea about particle dispersion by turbulence.

Conclusions

Computations for the chosen test cases of the FORTWIHR project have been presented. The simulations are for a confined jet with light and heavy particles. For all the cases, the agreements with the experimental data were in the range expected from other computations of these test cases. There are some slight discrepancies between the predictions and the experiments. This is probably partially a result of the deficiencies in the k-ε model to correctly predict heterogeneous effects in the flow. Another source of uncertainty is the inflow conditions, which were incomplete. A turbulent length scale distribution had to be assumed which might be partly responsible for the differences. In general, the agreement between the two codes was very good. This is the main result of these test computations, as it shows that the models are properly implemented and give a good agreement with the gas and particle velocities from the experiments.

There are, of course, still some general problems to be solved for improving calculation efficiency of two-phase flow and to make the numerical codes more efficient in order to allow the calculation of more complex flow in experimentally non-established situation with an acceptable confidence. In general, presented calculation results of the test cases showed a quite good agreement with the experimental data. This gives significant contribution to overcome existing uncertainties in two-phase flow prediction.

References

[1] *** ASC, TASCflow User Documentation, Version 2.4, Advanced Scientific Computing Ltd., Waterloo, Ontario, Canada, 1995

[2] Sommerfeld, M., Particle Laden Confined Jet Flow, *Proceedings*, Fifth Workshop on Two Phase Flow Predictions (Eds. M. Sommerfeld, D. Wennerberg), Erlangen, Germany, March 19–22, 1990, pp. 3–14

[3] Sommerfeld, M., Round Two-Phase Free Jet, *Proceedings*, Fourth Workshop on Two-Phase Flow Predictions (Eds. M. Sommerfeld, H. Zeisel), Erlangen, Germany, October, 1987, pp. 29–37

[4] Sommerfeld, M., Qiu, H.-H., Detailed Measurements in a Swirling Two-Phase Flow by a Phase-Doppler Anemometer, *Proceedings*, Fifth Workshop on Two Phase Flow Predictions (Eds. M. Sommerfeld, D. Wennerberg), Erlangen, Germany, March 19–22, 1990, pp. 15–31

[5] Ruck, B., Makiola, B., Particle Dispersion in a Single-Sided Backward-Facing Step Flow, *Int. J. Multiphase Flow*, *14* (1988), 6, pp. 787–800

[6] Hishida, K., Tabemoto, K., Meada, M., Turbulence Characteristics of Gas-Solid Two-Phase Confined Jet: Effect of Particle Density, *Japanese J. Multiphase Flow*, *1*, (1987), pp. 56–69

[7] Fleckhaus, D., Hishida, K., Meada, M., Turbulence Structure of Gas Solid Two-Phase Circular Jet, *Trans. Jap. Soc. Mech. Eng., 51-b* (1985), pp. 2330–2337

[8] Makgirk, J., Rodi, W., Calculation of the Three-Dimenssional Turbulent Jet, in: Turbulent Shear Flows (in Russian), Mashinostrenie, Moskva, 1982

[9] Rodi, W., A New Algebraic Relations for Calculating the Reynolds Stress, ZAMM 56, T219, 1976

[10] Launder, B. E., Second-Moment Closure: Methodology and Practice, au: Collection de la Direction des études et reshershes d'Électricité de France, Paris, 1984

[11] Sommerfeld, M., Particle Dispersion in Turbulent Flow: The Effect of Particle Size Distribution, Part. Syst. Charact. 7, 1990, pp. 209–220

[12] Hinze, J. O., Turbulence, McGraw-Hill, Inc., 1975

[13] Zou, L. X., Lin, W. Y., Sun, K. M., Simulation of Swirling Sudden-Expansion Gas-Particles Flows Using a k-ε-k_p Two-Phase Turbulence Model, *Proceeding*, 2nd International Conference on Multiphase Flow '95, Kyoto, Japan, 1995, pp. P3–75–P3–81

[14] Crowe, C. T., Review-Numerical Models for Dilute Gas-Particle Flows, *Journal of Fluids Engineering, Transactions of the ACME, 104* (1982), pp. 297

[15] Graham, D. I., Analytical Comparison of Lagrangian Particle Dispersion Models, Third International Conference on Multiphase Flows, Lion, France, June 1998
[16] Kenning, V. M., Crowe, C. T., Effect of Particles on Carrier Phase Turbulence in Gas Particles Flow, *Int. J. Multiphase Flow, 23* (1997), p. 403
[17] Sijerčić, M., Menter, F., Numerical Simulation of Two-Phase Flows in the FORTWIHR Research Program, Technical Report AEAT/TR-00-19, AEA Technology GmbH, Otterfing, Germany, 2000

Authors' addresses:

M. Sijerčić
Laboratory for Thermal Engineering and Energy,
VINČA Institute of Nuclear Sciences
P. O. Box 522, 11001 Belgrade, Yugoslavia
F. Menter
AEA Technology GmbH
Otterfing, Germany

Paper submited: September 1, 2000
Paper revised: November 15, 2000
Paper accepted: December 15, 2000